Colourimetric and spectroscopic discrimination between nucleotides and nucleosides using *para*-sulfonato-calix[4]arene capped silver nanoparticles

Yannick Tauran,[a] Marie Grosso,[a] Arnaud Brioude,[a] Rima Kassab[b] and Anthony W. Coleman*[a]

The complexation of nucleosides and nucleotides by hybrid nanoparticles capped by *para*-sulfonato-calix[4]arene shows clear discrimination between purine and pyrimidine based molecules. For the pyrimidine nucleotides there is appearance of a new absorption band around 550 nm, and a colour change from yellow to orange red and pink.

The calix[*n*]arenes are one of the most widely studied organic host classes.[1] In recent years their interactions with biological molecules,[2] and indeed their biochemistry[3,4] have been widely studied. In contrast to the large body of work on their complexation with amino acids,[5] peptides[6] or proteins[7] the study of their interactions with nucleosides,[8] nucleotides[9] and RNA[10] or DNA[11] is sparse. Generally the work has concentrated on coupling nucleosides onto the calix[*n*]arene skeleton,[12] although Goto *et al.* have studied the extraction of various nucleosides where a strong selectivity for adenine was observed.[13] The solid-state structures between *para*-sulfonato-calix[4]arene and the adeninium cation,[14] and also the mixed system guanine and cytosine,[15] have been reported.

Recently Xiong *et al.* have developed stable nanoparticles of silver or gold capped with *para*-sulfonato-calix[4]arene.[16,17] These have been shown to colourimetrically recognise amino acids with a high selectivity for histidine.

The use of metal nanoparticles for the complexation and detection of nucleic acids,[18] has received a large amount of attention, particularly as the method is sensitive enough to detect heavy metal ion induced DNA damage.[19]

In this communication we describe the interactions between nucleic bases and *para*-sulfonato-calix[4]arene capped silver nanoparticles. New absorbances at around 530 nm occur for pyrimidine bases accompanied by a colour shift from yellow to orange red and pink; these changes arise from nanoparticle aggregation.

The chemical structures of the nucleic bases and nucleotides are given in Scheme 1, in which it can be seen that the purines are composed of two heterocycles whereas the pyrimidines contain only one heterocycle.

The *para*-sulfonato-calix[4]arene capped silver nanoparticles, SC4:Ag NPs, were prepared by the method reported by Xiong *et al.*,[16] to these NPs were added solutions of the nucleic bases and nucleotides at a concentration of 10^{-2} M and then diluted to 10^{-3} M. The spectra were measured directly using a 96 titre well visible spectrometer.

The spectra are shown, at 1 hour after addition, in Fig. 1a–c and at 24 hours after addition, in Fig. 2a–c.

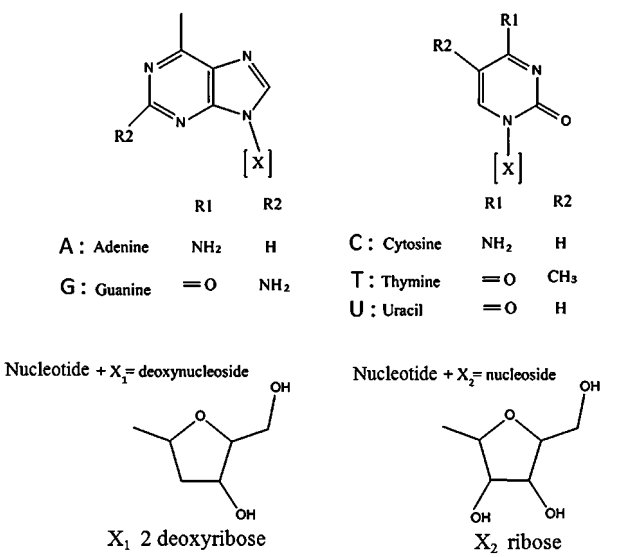

Scheme 1 Aromatic purine and pyrimidine ring structure of nucleotide bases. Differing side groups for all five different bases are indicated by R1 and R2. Deoxyribose or ribose conjugated with nucleotides gives deoxynucleoside or nucleoside.

[a] *LMI CNRS UMR 5615, Univ. Lyon 1, Villeurbanne, F69622, France. E-mail: antony.coleman@adm.univ-lyon 1.fr; Tel: +33 4 4243 1027*
[b] *University of Balamand, Faculty of Sciences, Department of Chemistry, P.O. Box: 100, Tripoli, Lebanon. E-mail: rima.kassab@balamand.edu.lb; Tel: +961 6 930250*

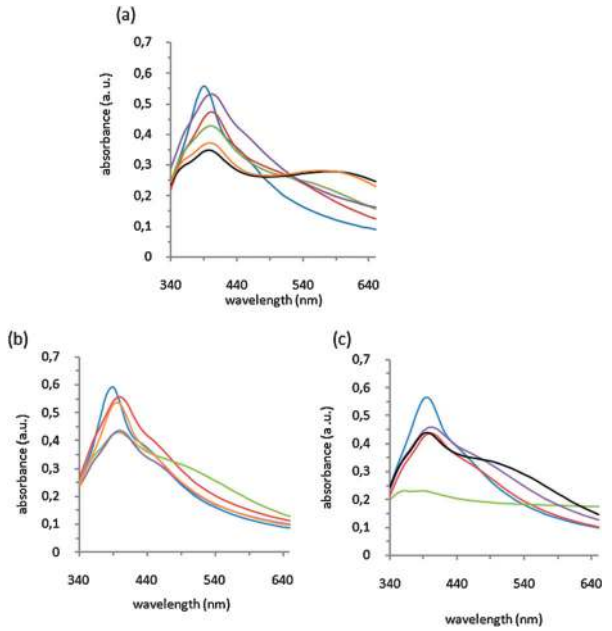

Fig. 1 Visible spectra of the complexation of (a) nucleotide, (b) nucleoside and (c) deoxy-nucleoside bases with SC4:Ag NPs after one hour at a final concentration of 10^{-3} M. Blue line: pSC4:Ag NP; red line: pSC4–Ag NP + A; purple line: pSC4–Ag NP + G; green line: pSC4–Ag NP + C; orange line: pSC4–Ag NP + U; black line: pSC4–Ag NP + T.

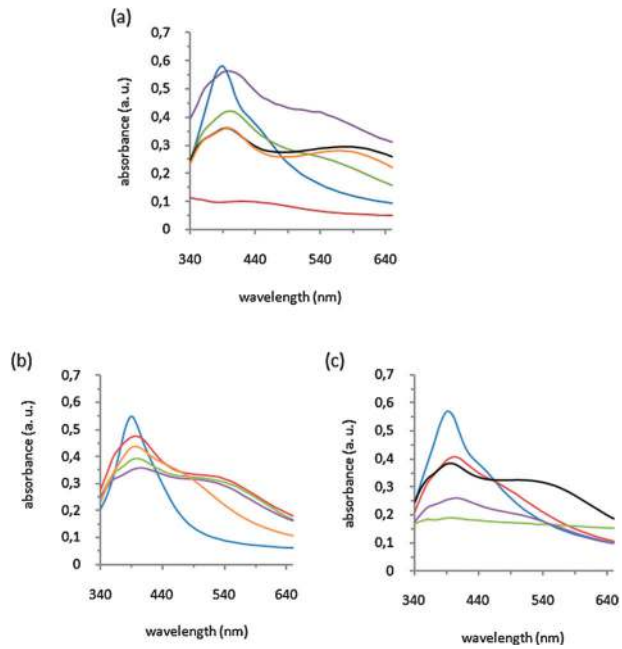

Fig. 2 Visible spectra of the complexation of (a) nucleotide, (b) nucleoside and (c) deoxy-nucleoside bases with SC4:Ag NPs after one hour at a final concentration of 10^{-3} M. Blue line: pSC4–Ag NP; red line: pSC4–Ag NP + A; purple line: pSC4–Ag NP + G; green line: pSC4–Ag NP + C; orange line: pSC4–Ag NP + U; black line: pSC4–Ag NP + T.

In Fig. 3 are given photographic images of the solutions. There are clear visible differences between the various nucleotides and nucleosides. For the nucleotides the pyrimidine bases are red to violet. For the nucleosides only cytosine leads to a visible change.

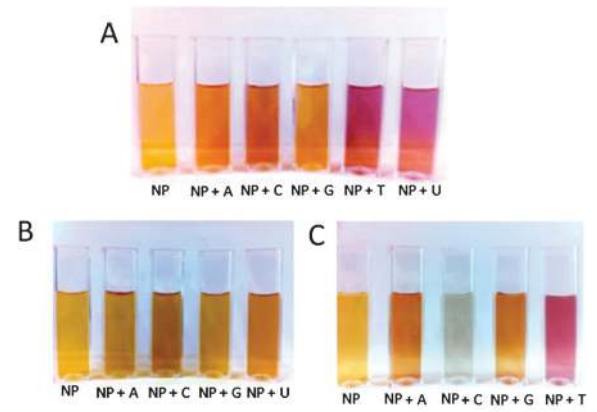

Fig. 3 Photographs of the complexation of (A) nucleotide, (B) nucleoside and (C) deoxy-nucleoside bases with SC4:Ag NPs after one hour at a final concentration of 10^{-3} M.

However for the deoxy-nucleotides with thymidine the solution turns violet and with cytosine there is a pale grey solution without the presence of the plasmon resonance.

With regard to the visible spectra a redshift occurs in the plasmonic absorption for all systems. This shift, see Table S1 (ESI†), indicates that there is complexation on the nanoparticle of the nucleotides, nucleosides and deoxy-nucleotides. The red shift of 10 nm is constant for all the systems studied here. Considering the thickness and the refractive index of layers formed at the metallic nanoparticles surface by those organic molecules, such behaviour is consistent with red shifts already observed in many systems.[20]

In the case of the nucleotides, after one hour for adenine and guanine, the spectra are essentially identical to the SC4:AgNPs. For cytosine a second peak appears at 540 nm, now for thymine and uracil this peak is strongly red shifted to 580 nm. After 24 hours the situation has again changed considerably; now for guanine a peak appears at 540 nm, while the peak for the cytosine complex remains at 540 nm. The peak arising from uracil remains at 580 nm while that for thymine shifts slightly to 590 nm. Intriguingly for adenine after 24 hours a clear solution of SC4:AgNPs was obtained, this is a highly reproducible phenomenon.

This effect is of considerable interest as cytosine and thymidine are present in RNA and DNA whereas uracil is present only in RNA. This suggests a possible spectroscopic means of determining RNA and DNA contents.

For the nucleosides after 1 hour, a second peak at higher wavelength appears at 450 nm for adenosine, uridine, guanosine and at 490 nm for cytidine. Such plasmon resonance bands can be attributed to the formation of metallic nanoparticle aggregates.[20] The situation changes radically after 24 hours now in all cases there is the presence of a peak at 520 nm except for uridine where the band is shifted to 470 nm. Thus it is possible to discriminate between the two sets of nucleosides by the kinetics of their aggregation behaviour.

With regard to the deoxy-nucleosides, after one hour, the behaviour is somewhat different, again there is a red shift in the peaks associated with the plasmon resonance. For deoxy-adenosine and deoxy-guanosine an aggregation peak at 460 nm is present. The aggregation peak of deoxy-thymidine has been

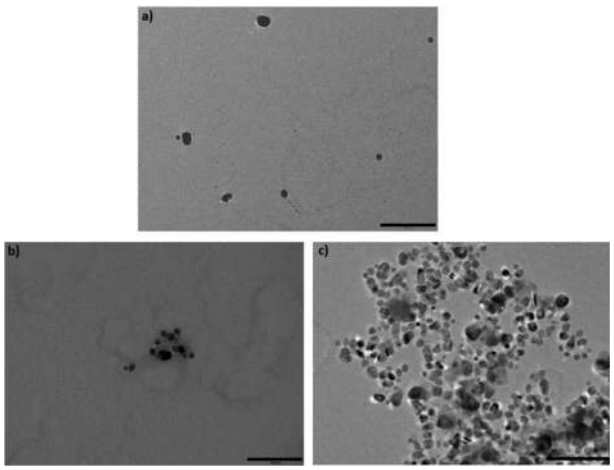

Fig. 4 TEM images of pSC4–Ag NPs (a) alone, (b) after addition of adenosine at a final concentration of 10^{-3} M, (c) after addition of thymidine at a final concentration of 10^{-3} M. The scale bars are for all pictures 100 nm.

strongly red-shifted to 520 nm. However for the mixture of SC4:AgNPs with deoxy-cytidine the result is the loss of all peaks and the solution turns grey.

In general, there is also appearance of weak peaks and shoulders in the region of 360 nm which may be attributed to the presence of multipolar plasmon resonances (quadrupolar mode). This particular resonance is well-known in the silver case for nanoparticles size greater than 50 nm.[21]

Transmission electron microscopy, as shown above in Fig. 4, confirms the aggregation caused by deoxy-nucleosides. It can be clearly seen that the SC4:AgNPs are present alone as well separated objects around 20 nm in size. For adenosine where the spectrum shows a weak peak for the aggregation of small clumps of the nanoparticles is present. However in the case of thymidine where a strong peak at 540 nm is observed and there is a colour change to pink, the nanoparticles are strongly aggregated. Dynamic light scattering shows a population at 30 nm for SC4:AgNPs and for the thymidine complexed SC4:AgNPs a high degree of polydispersity is observed with populations up to 300 nm in diameter. For the less aggregated systems in addition to single particles there are in general populations of about 100 nm in diameter.

For the SC6:AgNPs and the SC8:NPs the situation is very different, here there is in most cases the 10 nm red shift, ESI† figures, but no aggregation takes place and hence no peaks are observed in the region 500–600 nm and no colour changes are observed.

The results obtained point to an association between the various types of nucleotides and nucleosides with the cavity of *para*-sulfonatocalix[4]arene, that is inconsistent with the proposition of Xiong *et al.*[16] where the *para*-sulfonatocalix[4]arene molecules coordinate to the NPs *via* the sulfonate groups thus blocking the cavity. A more reasonable explanation lies in the formation of the classic bilayer solid-state structure,[22] where alternate coordinated *para*-sulfonatocalix[4]arene molecules and available cavities are present at the surface of the

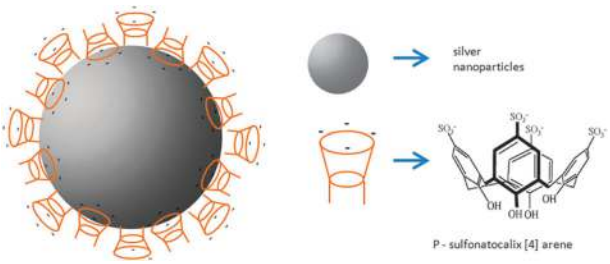

Fig. 5 Schematic representation of the organization of *para*-sulfonatocalix[4]arene on silver nanoparticles.

nanoparticles, as shown in Fig. 5. This would be associated with a population of between 400 and 1000 molecules at the SC4:AgNPs surface.

In conclusion we have shown that the interactions of SC4:AgNPs with nucleotides, nucleosides and deoxy-nucleosides yield selective complexation reflected both in changes in colour and in the visible spectrum due to aggregate formation.

Notes and references

1 C. D. Gutsche, *Calixarenes an Introduction, 2nd edn*, The Royal Society of Chemistry, Cambridge, 2008.
2 R. V. Rodik, V. I. Boyko and V. Kalchenko, *Curr. Med. Chem.*, 2009, **16**, 1630–1655.
3 A. W. Coleman, F. Perret, A. Moussa, M. Dupin, Y. Gu and H. Perron, *Top. Curr. Chem.*, 2007, **277**, 31–88.
4 F. Perret, A. N. Lazar and A. W. Coleman, *Chem. Commun.*, 2006, 2425–2438.
5 E. Da Silva and A. W. Coleman, *Tetrahedron*, 2003, **59**, 7357–7364.
6 N. Douteau-Guevel, F. Perret, A. W. Coleman, J. P. Morel and N. Morel-Desrosiers, *J. Chem. Soc., Perkin Trans. 2*, 2002, 524–532.
7 R. Zadmard and T. Schrader, *J. Am. Chem. Soc.*, 2005, **127**, 904–915.
8 F. Sansone, L. Baldini, A. Casnati and R. Ungaro, *New J. Chem.*, 2010, **34**, 2715–2728.
9 G. M. L. Consoli, G. Granata, R. Lo Nigro, G. Malandrino and C. Geraci, *Langmuir*, 2008, **24**, 6194–6200.
10 R. Zadmard and T. Schrader, *Angew. Chem., Int. Ed.*, 2006, **45**, 2703–2706.
11 S. J. Kim and B. H. Kim, *Tetrahedron Lett.*, 2002, **43**, 6367–6371.
12 G. M. L. Consoli, G. Granata, D. Garozzo, T. Mecca and C. Geraci, *Tetrahedron Lett.*, 2007, **48**, 7974–7977.
13 K. Shimojo, T. Oshima and M. Goto, *Anal. Chim. Acta*, 2004, **521**, 163–171.
14 J. L. Atwood, L. J. Barbour, E. S. Dawson, P. C. Junk and J. Kienzle, *Supramol. Chem.*, 1996, **7**, 271–274.
15 P. J. Nichols, M. Makha and C. L. Raston, *Cryst. Growth Des.*, 2006, **6**, 1161–1167.
16 D. Xiong, M. Chen and H. Li, *Chem. Commun.*, 2008, 880–882.
17 T. T. Jiang, R. R. Liu, X. F. Huang, H. J. Feng, W. L. Teo and B. G. Xing, *Chem. Commun.*, 2009, 1972–1974.
18 Y. Cai, J. Wang, Y. Xu and G. Li, *Biosens. Bioelectron.*, 2010, **25**, 1032–1036.
19 Q. Zhang, P. Dai and Z. Yang, *Microchim. Acta*, 2011, **173**, 347–352.
20 D. D. Lekeufack, A. Brioude, A. W. Coleman, P. Miele, J. Bellessa, L. D. Zeng and P. Stadelmann, *Appl. Phys. Lett.*, 2010, **96**, 253107.
21 K. L. Kelly, E. Coronado, L. L. Zhao and G. C. Schatz, *J. Phys. Chem. B*, 2003, **107**, 668–677.
22 A. W. Coleman, S. G. Bott, D. S. Morley, C. M. Means, K. D. Robinson, H. Zhang and J. L. Atwood, *Angew. Chem., Int. Ed. Engl.*, 1988, **27**, 1361–1362.